bioRxiv preprint doi: https://doi.org/10.1101/763227; this version posted September 9, 2019. The copyright holder for this preprint (which was not certified by peer review) is the author/funder. All rights reserved. No reuse allowed without permission.

Repression of Viral Gene Expression and Replication by the Unfolded Protein Response Effector XBP1u

Florian Hinte[1], Eelco van Anken[2,3], Boaz Tirosh[4], Wolfram Brune[1,*]

1 Heinrich Pette Institute, Leibniz Institute for Experimental Virology, Hamburg, Germany
2 Division of Genetics and Cell Biology, San Raffaele Scientific Institute, Milan, Italy
3 Università Vita-Salute San Raffaele, Milan, Italy
4 Institute for Drug Research, School of Pharmacy, Faculty of Medicine, The Hebrew University, Jerusalem, Israel
* Corresponding author. Phone: +49 40 48051351; Email: wolfram.brune@leibniz-hpi.de

Running title: Cytomegalovirus repression by XBP1u

Word count
Abstract: 165
Text: 4969

bioRxiv preprint doi: https://doi.org/10.1101/763227; this version posted September 9, 2019. The copyright holder for this preprint (which was not certified by peer review) is the author/funder. All rights reserved. No reuse allowed without permission.

Abstract

The unfolded protein response (UPR) is a cellular homeostatic circuit that regulates protein synthesis and processing in the ER by activating three ER-to-nucleus signaling pathways. One of these pathways is triggered by the inositol-requiring enzyme 1 (IRE1), which splices the X-box binding protein 1 (XBP1) mRNA, thereby enabling the expression of the transcription factor XBP1s. Another UPR pathway triggers proteolytic activation of the activating transcription factor 6 (ATF6). Here we show that murine cytomegalovirus (MCMV), a prototypic β-herpesvirus, harnesses the UPR to regulate its own life cycle. MCMV transiently activates the IRE1-XBP1 pathway early post infection in order to relieve repression by XBP1u, the product of the unspliced *Xbp1* mRNA. XBP1u inhibits viral gene expression and replication by blocking the activation of the viral major immediate-early promoter by XBP1s and ATF6. These findings reveal a redundant function of XBP1s and ATF6 as activators of viral gene expression and replication, and an unexpected role of XBP1u as a potent repressor of both XBP1s and ATF6-mediated activation.

Key words: unfolded protein response / transcription factor / XBP1u / ATF6 / cytomegalovirus.

Introduction

The endoplasmic reticulum (ER) is responsible for synthesis, posttranslational modification, and folding of a substantial portion of cellular proteins. When protein synthesis is increased or ER function is compromised, the folding capacity of the ER may get out of balance, leading to an accumulation of unfolded or misfolded proteins in the ER. To alleviate ER stress and restore homeostasis, the cell activates three ER-to-nucleus signaling pathways, collectively called the unfolded protein response (UPR), which lead to a reduced protein synthesis and an increased expression of folding chaperones and ER-associated degradation (ERAD) factors (Walter & Ron, 2011). Subsequently, ER folding capacity increases and terminally misfolded protein species are exported from the ER and targeted for proteasomal degradation (Christianson & Ye, 2014).

In mammalian cells, the UPR comprises three main signaling pathways named after the initiating ER stress sensors: PERK (PKR-like ER kinase), ATF6 (activating transcription factor 6), and IRE1 (inositol-requiring enzyme 1) (Walter & Ron, 2011). Upon activation by ER stress, PERK phosphorylates the translation initiation factor eIF2α, which leads to a massive attenuation of protein synthesis and an immediate reduction of the protein load in the secretory system. However, phosphorylated eIF2α selectively supports the translation of

bioRxiv preprint doi: https://doi.org/10.1101/763227; this version posted September 9, 2019. The copyright holder for this preprint (which was not certified by peer review) is the author/funder. All rights reserved. No reuse allowed without permission.

selected cellular proteins such as the transcription factor ATF4, which activates a negative feedback loop resulting in dephosphorylation of eIF2α (Novoa et al, 2001).

Upon activation by ER stress, ATF6 travels to the Golgi, where it undergoes intramembrane proteolysis. This process liberates its cytosolic N-terminus, the basic leucine zipper (bZIP) transcription factor ATF6(N), and enables it to travel to the nucleus, where it activates the transcription of chaperone genes as well as of the gene encoding XBP1 (Lee et al, 2002).

The third sensor, IRE1, is an ER transmembrane protein kinase that oligomerizes upon accumulation of unfolded proteins in the ER lumen. Oligomerization and auto-transphosphorylation activates the RNase function of IRE1, which mediates an unconventional splicing of the XBP1 mRNA in the cytosol (Calfon et al, 2002; Lee et al, 2002; Yoshida et al, 2001). Removal of the 26-nt intron from the XBP1 mRNA leads to a frame shift and expression of transcription factor XBP1s, comprising an N-terminal basic leucine zipper (bZIP) domain followed by a C-terminal transcription activation domain. In contrast, the unspliced XBP1 mRNA encodes XBP1u, which lacks the transcription activation domain but contains a hydrophobic patch in the C-terminal part. XBP1u is rapidly degraded and has a short half-life (Tirosh et al, 2006). It can interact with XBP1s and ATF6(N) and target them for proteasomal degradation. Therefore, XBP1u is thought acts as a negative regulator involved in fine-tuning the UPR (Tirosh et al, 2006; Yoshida et al, 2006; Yoshida et al, 2009). Moreover, XBP1u affects autophagy by interacting with transcription factor FOXO1 (Zhao et al, 2013). Apart from mediating XBP1 mRNA splicing, IRE1 can also cleave ER-associated mRNA molecules that contain a specific recognition motif (Moore & Hollien, 2015). This process, which leads to mRNA degradation, is called regulated IRE1-dependent mRNA decay (RIDD). However, the importance of RIDD in different cellular processes such as lipid metabolism, antigen presentation, and apoptosis remains incompletely understood (Maurel et al, 2014).

During viral replication large quantities of viral proteins must be synthesized. Folding, maturation, and posttranslational modification of secreted and transmembrane proteins take place in the ER and require a plethora of chaperones, foldases, and glycosylating enzymes. While properly folded proteins are transported to the Golgi, unfolded or misfolded proteins are retained in the ER and exported to the cytosol for proteasomal degradation via the ER-associated protein degradation (ERAD) pathway (Smith et al, 2011). However, the high levels of viral envelope glycoproteins that are being synthesized particularly during the late phase of the viral life cycle can overwhelm the folding and processing capacity of the ER and cause accumulation of unfolded and misfolded proteins in the ER (Zhang & Wang, 2012).

Cytomegaloviruses (CMVs) are prototypic members of the β subfamily of the *Herpesviridae*. Their large double-stranded DNA genomes contain at least 165 protein-

bioRxiv preprint doi: https://doi.org/10.1101/763227; this version posted September 9, 2019. The copyright holder for this preprint (which was not certified by peer review) is the author/funder. All rights reserved. No reuse allowed without permission.

coding ORFs (Dolan et al, 2004) end encode an even larger number of polypeptides (Stern-Ginossar et al, 2012). Through millions of years of co-evolution with their respective hosts, the CMVs have acquired the ability to moderate immune recognition and modulate cellular stress responses to their own benefit (Alwine, 2008; Mocarski, 2002). Considering the important role of the UPR in controlling cell fitness, it is hardly surprising that the CMVs have evolved means to modify the UPR. For instance, human and murine CMV (HCMV and MCMV) induce PERK activation, but limit eIF2α phosphorylation. By doing this the CMVs prevent a global protein synthesis shutoff but allow eIF2α phosphorylation-dependent activation of transcription factor ATF4 (Isler et al, 2005; Qian et al, 2012). The CMVs also increase expression of the ER chaperone BiP to facilitate protein folding and virion assembly (Buchkovich et al, 2008; Buchkovich et al, 2010; Qian et al, 2012), and HCMV uses PERK to induce lipogenesis by activating the cleavage of sterol regulatory element binding protein 1 (Yu et al, 2013). We have previously shown that both, MCMV and HCMV, downregulate IRE1 levels and inhibit IRE1 signaling at late times post infection. This downregulation is mediated by the viral proteins M50 and UL50, respectively (Stahl et al, 2013). However, a real-time transcriptional profiling study has revealed that cellular ER stress response transcripts are upregulated as early 5-6 hours after MCMV infection (Marcinowski et al, 2012).

Here we show that MCMV transiently activates the IRE1-XBP1 pathway at early times postinfection in order to relieve repression of viral gene expression and replication by XBP1u. When IRE1-mediated XBP1 mRNA splicing is inhibited, XBP1u blocks the activation of the viral major immediate-early promoter (MIEP) by XBP1s and ATF6(N). Thus, MCMV exploits UPR signaling to boost the activity of its most important promoter. Moreover, these findings reveal a redundant function of XBP1s and ATF6 as activators of viral gene expression and replication, and an unexpected role of XBP1u as a potent repressor of both XBP1s and ATF6-mediated activation.

Results

Early activation of IRE1-XBP1 signaling promotes MCMV replication.

Previous studies have shown that MCMV inhibits IRE1-XBP1 signaling at late times (≥24 h) post infection (Qian et al, 2012; Stahl et al, 2013). However, cellular ER stress response transcripts were shown to be upregulated at 5-6 hours after MCMV infection (Marcinowski et al, 2012), suggesting that UPR signaling is activated at early times post infection. Thus, we decided to analyze whether MCMV activates the IRE1-XPB1 signaling pathway within the first few hours after infection. To do this, we infected mouse embryonic fibroblasts (MEFs) with MCMV and quantified spliced and unspliced XBP1 transcripts by qRT-PCR. We detected a short and transient increase of XBP1 splicing between 5 and 7 hours post

bioRxiv preprint doi: https://doi.org/10.1101/763227; this version posted September 9, 2019. The copyright holder for this preprint (which was not certified by peer review) is the author/funder. All rights reserved. No reuse allowed without permission.

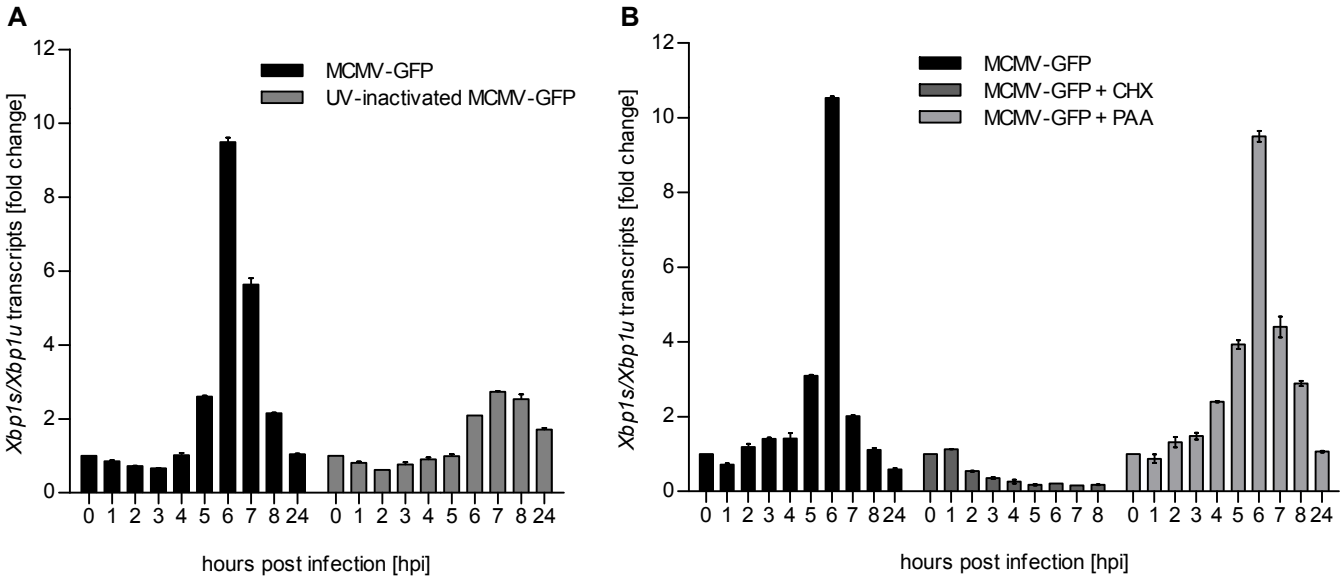

Figure 1.
MCMV induces *Xbp1s* mRNA splicing at early time of infection

A. MEFs were infected with MCMV-GFP or UV-inactivated MCMV-GFP (MOI 4). Cells were harvested at the indicated times, total RNA was extracted, and *Xbp1s* and *Xbp1u* transcripts were quantified by qPCR. Changes in the *Xbp1s/Xbp1u* ratio relative to uninfected cells are plotted as bar diagram (means ±SEM of triplicates).

B. MEFs were infected with MCMV-GFP as described above and treated with vector, CHX (50µg/ml) or PAA (250ng/ml). Changes in the *Xbp1s/Xbp1u* ratio were determined as described above.

bioRxiv preprint doi: https://doi.org/10.1101/763227; this version posted September 9, 2019. The copyright holder for this preprint (which was not certified by peer review) is the author/funder. All rights reserved. No reuse allowed without permission.

infection (hpi) (Fig. 1A). This increase was massively reduced when cells were infected with UV-inactivated MCMV (Fig. 1A), suggesting that XBP1 splicing was not caused by viral attachment and entry into cells but required viral gene expression. MCMV-induced XBP1 splicing was also suppressed by cycloheximide (CHX, a translation inhibitor), but not by phosphonoacetic acid (PAA), an inhibitor of viral DNA replication and late gene expression (Fig. 1B). These results suggested that the transient activation of the IRE1-XBP1 pathway is caused by viral proteins expressed at immediate-early or early times post infection.

To determine whether IRE1 signaling is important for the MCMV life cycle, we used *Ire1*$^{-/-}$ cells expressing IRE1-GFP under tight control of a tetracycline-inducible promoter (Fig. 2A) for analyses of viral replication. IRE1-GFP expression was induced with different concentrations of doxycycline, and cells were infected at low or high multiplicity of infection (MOI) for multi-step and single-step growth curves, respectively (Fig. 2B and C). In both types of replication analysis, MCMV replicated to low titers when IRE1 expression was induced with very low or very high doxycycline concentrations. High MCMV titers (~10^6 infectious units per ml), comparable to those obtained in wildtype (WT) MEFs, were attained only upon moderate induction of IRE1-GFP with 5 to 10 nM doxycycline (Fig. 2B and C). Thus we concluded that IRE1 is necessary for efficient replication of MCMV, but needs to be carefully regulated as too high expression levels are detrimental for viral replication.

IRE1, but not XBP1 or TRAF2, is required for efficient MCMV gene expression and replication.

Activated IRE1 can splice *Xbp1* mRNA (Calfon et al, 2002; Lee et al, 2002; Yoshida et al, 2001) and can also recruit TRAF2 to activate ASK1 (Urano et al, 2000). To test which IRE1-dependent signaling pathway is required for efficient MCMV replication, we used CRISPR/Cas9-mediated gene editing to generate *Ire1* knockout (ko), *Xbp1* ko, and *Traf2* ko MEFs. For each gene knockout, two independent cell clones were generated with different guide RNAs. The absence of the respective gene products was verified by immunoblot analysis (Fig. 3A). Then the cell clones were used to assess MCMV replication. In *Ire1* ko MEFs, viral replication was reduced by two orders of magnitude as compared to WT MEFs (Fig. 3B), similar to the reduction seen in IRE1-GFP cells without doxycycline induction (Fig. 2B). By contrast, MCMV replication was virtually unimpaired in the absence of *Xbp1* (Fig. 3B) or *Traf2* (Fig. 3C). We also analyzed the expression of a viral immediate-early (IE1), an early (M57), and a late protein (gB) at different times post infection. Compared to WT MEFs, the expression of all three proteins was reduced in *Ire1* ko MEFs (Fig. 3D), but not in *Xbp1* or *Traf2* ko MEFs (Fig. 3E and F).

Next we tested whether the RNAse activity of IRE1 is required for efficient MCMV replication. To do this, WT IRE1 or an "RNAse-dead" IRE1 K907A mutant (Tirasophon et al,

bioRxiv preprint doi: https://doi.org/10.1101/763227; this version posted September 9, 2019. The copyright holder for this preprint (which was not certified by peer review) is the author/funder. All rights reserved. No reuse allowed without permission.

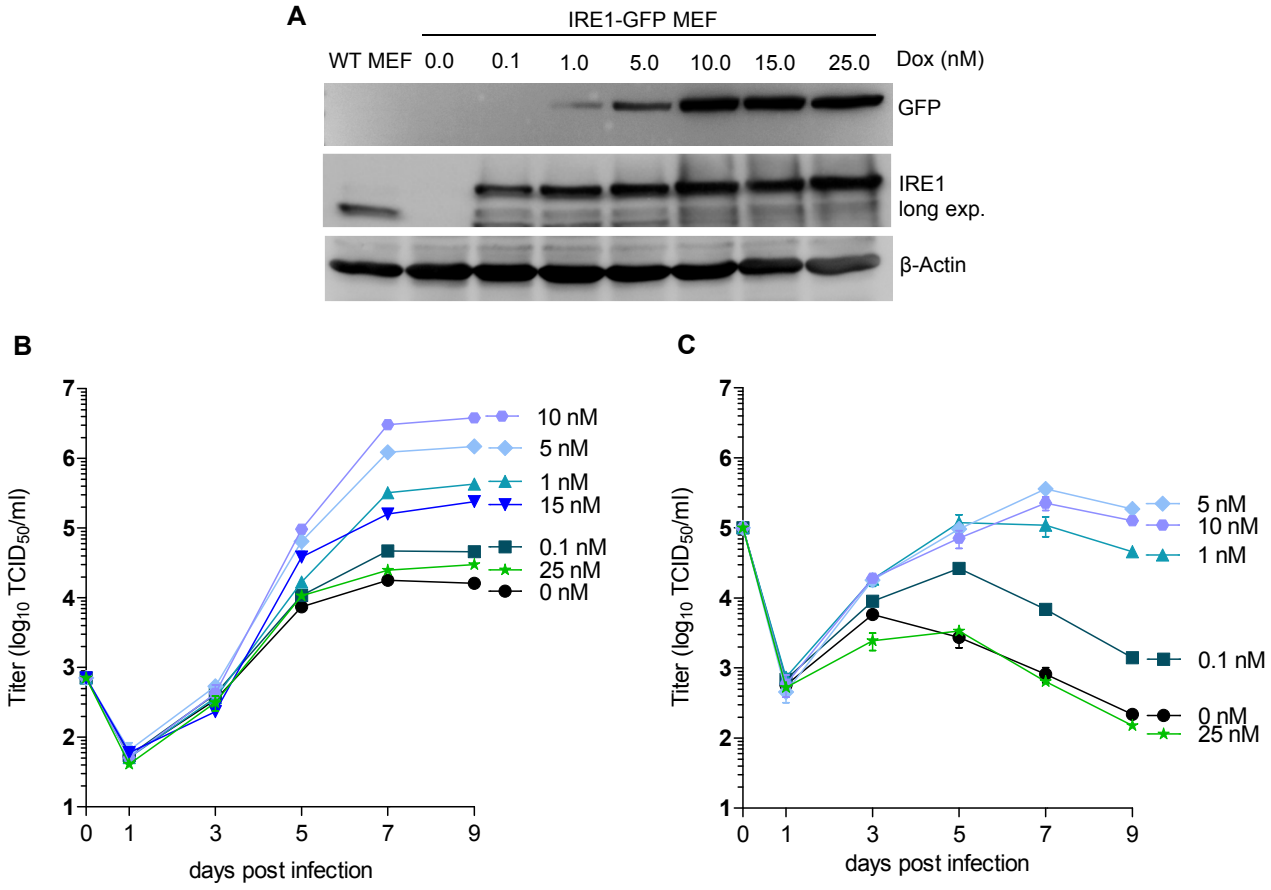

Figure 2.
Moderate IRE1 expression is beneficial for MCMV replication.

A. Immunoblot analysis of *Ire1*$^{-/-}$ MEFs expressing IRE1-GFP in a doxycycline (dox)-inducible manner. Cells were treated with different dox concentrations for 24 h. IRE1-GFP expression was detected with GFP or IRE1-specific antibodies. Endogenous IRE1 levels in WT MEFs were detected only with the IRE1-specific antibody.

B. Multistep MCMV replication kinetics on IRE1-GFP MEFs induced with different dox concentrations. 24 h after induction, cells were infected with MCMV-GFP (MOI 0.1). Virus titers in the supernatants were determined by titration and are shown as means ±SEM of triplicates.

C. Single step MCMV replication kinetics on IRE1-GFP MEFs induced with dox as above and infected with MCMV-GFP (MOI 3).

bioRxiv preprint doi: https://doi.org/10.1101/763227; this version posted September 9, 2019. The copyright holder for this preprint (which was not certified by peer review) is the author/funder. All rights reserved. No reuse allowed without permission.

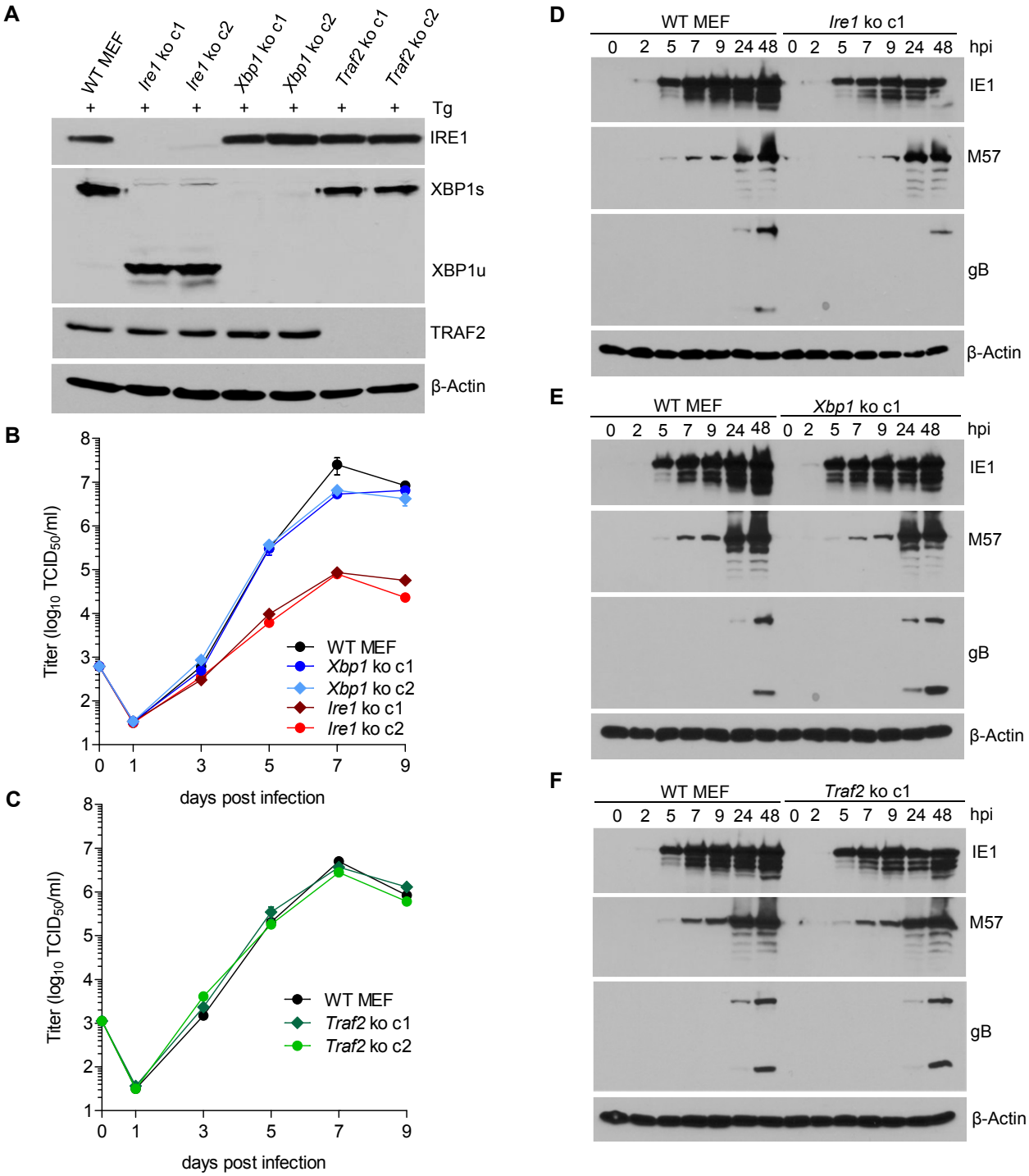

Figure 3.

IRE1, but not XBP1 or TRAF2, is required for efficient MCMV replication and viral protein expression

A. Immunoblot analysis of *Ire1*, *Xbp1* and *Traf2* ko cell lines. Two ko clones were generated for each gene by CRISPR/Cas9 gene editing using different gRNAs. Cells were treated for 4 h with Thapsigargin (Tg) to induce *Xbp1* mRNA splicing and to increase XBP1 expression.

B,C. Multistep MCMV replication kinetics in *Ire1*, *Xbp1* and *Traf2 ko* cells, respectively. Cells were infected with MCMV-GFP (MOI 0.1) Virus titers in the supernatants were determined by titration and are shown as means ±SEM of triplicates.

D-F. Immunoblot analysis of viral protein expression kinetics in *Ire1*, *Xbp1* and *Traf2 ko* cells, respectively. Cells were infected with MCMV-GFP (MOI 3) and harvested at different times post infection. Expression levels of the viral immediate-early 1 (IE1) protein, the major DNA binding protein (M57; an early protein), and glycoprotein B (gB; a late protein) were detected with specific antibodies, β-Actin served as loading control.

bioRxiv preprint doi: https://doi.org/10.1101/763227; this version posted September 9, 2019. The copyright holder for this preprint (which was not certified by peer review) is the author/funder. All rights reserved. No reuse allowed without permission.

2000) was expressed in *Ire1* ko MEFs by retroviral transduction. Expression of WT and mutant IRE1 and the ability to splice *Xbp1* was verified by immunoblot analysis (Fig. 4A). While expression of WT IRE1 restored MCMV replication to high titers, expression of IRE1 K907A did not increase MCMV titers (Fig. 4B), indicating that the IRE1 RNase activity is necessary for efficient MCMV replication.

XBP1u inhibits MCMV replication.

Our observations that the RNase activity of IRE1 is required for efficient MCMV replication, but XBP1 is not, allowed two possible explanations: (i) MCMV replication could benefit from RIDD, another RNase-dependent function of IRE1. However, this possibility is difficult to verify as selective inactivation of RIDD is complicated. (ii) Alternatively, MCMV replication could be inhibited by XBP1u, the product of the unspliced *Xbp1* mRNA, since *Ire1* ko cells differ from other cells in that they express only XBP1u (Fig. 3A). To test the latter option, we used two experimental approaches. First, we knocked out *Ire1* in *Xbp1*-deficient cells (Fig. 5A). As shown in figure 5B, MCMV replicated to similar titers in *Xbp1* ko and *Xbp1*/*Ire1* double-knockout (dko) cells, indicating that the loss of IRE1 is not detrimental for MCMV replication when XBP1 is absent. Next, we used retroviral transduction to restore XBP1 expression in $Xbp1^{-/-}$ cells. The retroviral vectors expressed the WT *Xbp1* transcript (which can be spliced by IRE1), a truncated *Xbp1* transcript encoding only the DNA-binding domain, or an 'unspliceable' *Xbp1* transcript. Upon treatment with thapsigargin, these cells expressed XBP1s, XBP1stop, or XBP1u, respectively (Fig. 5C). Whereas re-introduction of WT XBP1 had no detrimental effect, MCMV replication was severely impaired upon expression of the unspliceable *Xbp1* transcript (Fig. 5D), indicating that *Xbp1u* reduces viral replication. A similar inhibitory effect was observed when the truncated XBP1 (XBP1stop) protein was expressed (Fig. 5D).

Loss of XBP1 and ATF6 impairs MCMV replication.

XBP1u is thought to function as a negative regulator to XBP1s (Tirosh et al, 2006; Yoshida et al, 2006). However, the inhibition of MCMV replication by XBP1u cannot be explained solely by a repressive effect on XBP1s as a complete loss of XBP1 is not detrimental to MCMV replication in vitro (Fig. 3B) and has only a modest effect on viral replication in vivo (Drori et al, 2014). Thus we hypothesized that XBP1u might impair MCMV replication by repressing the activity of additional transcription factors besides XBP1s. For several reasons ATF6 appeared to be a likely target of XBP1u: (i) Like XBP1s, ATF6 is a bZIP transcription factor activated by ER stress (Yoshida et al, 1998); (ii) XBP1s and ATF6 are known to synergize in the activation of numerous ER stress response genes (Lee et al, 2002); and (iii) XBP1u can interact with ATF6 and inhibit its activity (Yoshida et al, 2009). Therefore, we tested whether

bioRxiv preprint doi: https://doi.org/10.1101/763227; this version posted September 9, 2019. The copyright holder for this preprint (which was not certified by peer review) is the author/funder. All rights reserved. No reuse allowed without permission.

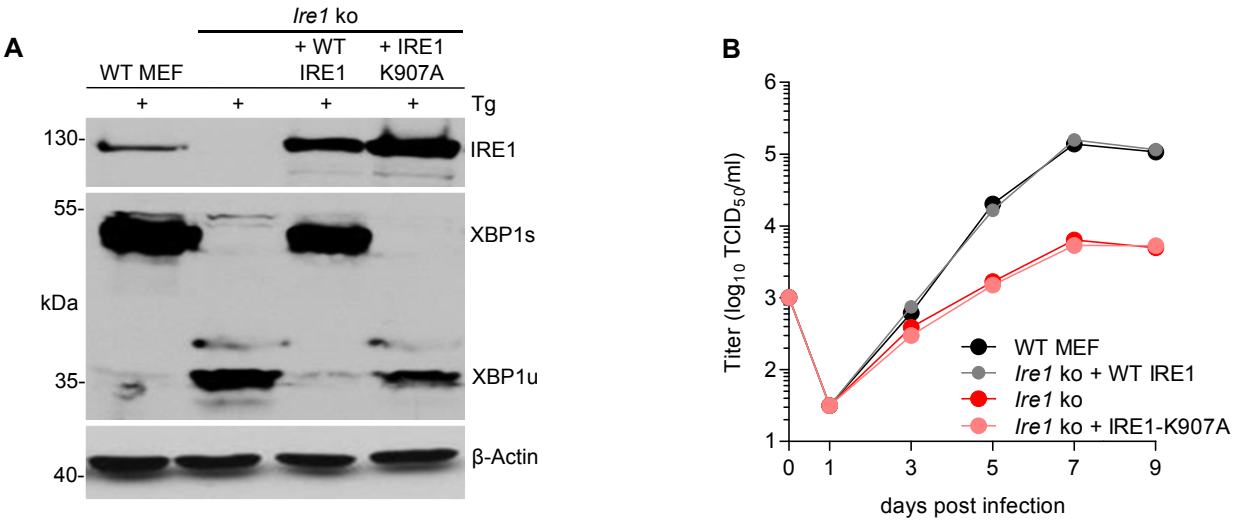

Figure 4.

The RNase function of IRE1 is required for efficient MCMV replication.

A. Immunoblot analysis of *Ire1* ko transduced with retroviral vectors expressing WT IRE1 or IRE1-K907A (RNase-dead). Cells were treated for 4 h with Thapsigargin (Tg) to induce *Xbp1* mRNA splicing and to increase XBP1 expression. IRE1 and XBP1 protein expression was detected by immunoblot.

B. Multistep MCMV replication kinetics in *Ire1 ko* cells complemented with WT IRE1 or IRE1-K907A, respectively. Cells were infected with MCMV-GFP (MOI 0.1). Virus titers in the supernatants were determined by titration and are shown as means ±SEM of triplicates.

bioRxiv preprint doi: https://doi.org/10.1101/763227; this version posted September 9, 2019. The copyright holder for this preprint (which was not certified by peer review) is the author/funder. All rights reserved. No reuse allowed without permission.

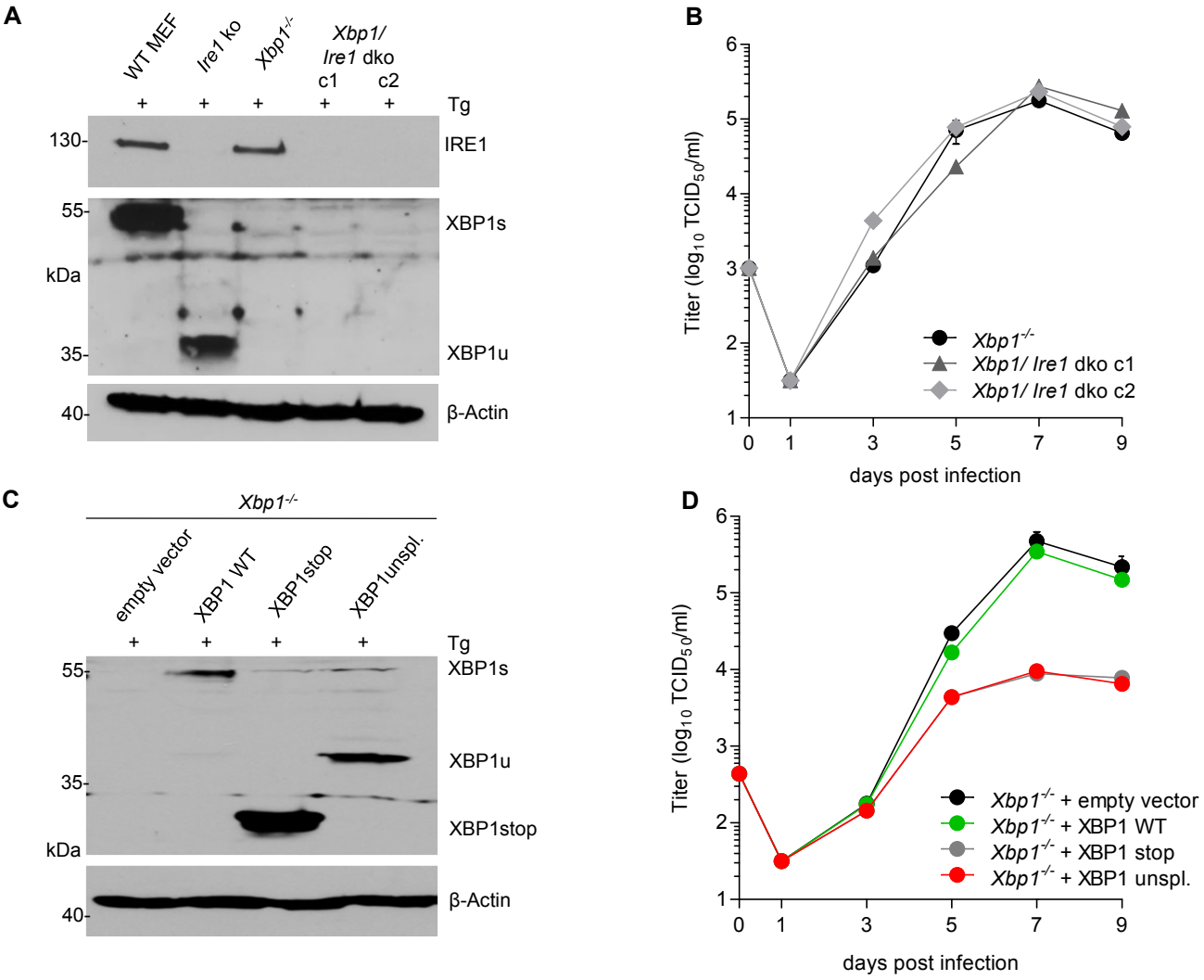

Figure 5.
XBP1u acts as a repressor for MCMV replication.

A. *Xbp1*$^{-/-}$ MEFs were used to knock out *Ire1* by CRISPR/Cas9 gene editing. Two double ko (dko) cell clones were generated with different gRNAs. IRE1 and XBP1 protein expression in the two dko clones and control cells was detected by immunoblot analysis. Cells were treated for 4 h with Thapsigargin (Tg) to induce *Xbp1* mRNA splicing and to increase XBP1 expression.

B. Multistep MCMV replication kinetics in *Xbp1*$^{-/-}$ and *Xbp1/Ire1* dko MEFs. Cells were infected with MCMV-GFP (MOI 0.1) Virus titers in the supernatants were determined by titration and are shown as means ±SEM of triplicates.

C. Immunoblot analysis of *Xbp1*$^{-/-}$ MEF transduced with retroviral vectors expressing a WT (spliceable) *Xbp1* transcript, an unspliceable *Xbp1* transcript, or a truncated (*Xbp1*stop) transcript. Cells were treated with Tg as described in A.

D. Multistep MCMV replication kinetics in cells shown in C. Infection and titration was done as in B.

bioRxiv preprint doi: https://doi.org/10.1101/763227; this version posted September 9, 2019. The copyright holder for this preprint (which was not certified by peer review) is the author/funder. All rights reserved. No reuse allowed without permission.

the loss of both, XBP1 and ATF6, was detrimental for MCMV replication. First, we analyzed MEFs from *Atf6*$^{-/-}$ mice and found that MCMV gene expression and replication were not impaired (Fig. 6A and B). When we knocked out *Xbp1* in *Atf6*$^{-/-}$ cells by CRISPR/Cas9 gene editing (Fig. 6C), MCMV replication was substantially reduced in *Atf6*/*Xbp1* dko cells (Fig. 6D), suggesting that ATF6 and XBP1s have overlapping or redundant functions and that at least one of them is necessary for efficient MCMV replication.

XBP1s and ATF6-mediated activation of the MCMV major immediate-early promoter (MIEP) is repressed by XBP1u.

The MCMV MIEP has a key role in viral gene expression as it drives the expression of the viral IE1 and IE3 proteins. IE3 is the major transactivator protein that activates early and late gene expression (Lacaze et al, 2011). Thus we interrogated whether XBP1s and ATF6 can activate the MCMV MIEP. First, we searched for ACGT motifs within the MCMV MIEP. ACGT is a minimal consensus sequence contained within XBP1s and ATF6 binding motifs (Kanemoto et al, 2005; Wang et al, 2000). Five ACGT motifs were identified within the MCMV MIEP. To analyze the function of these putative transcription factor binding sites, we inserted the WT MIEP and six mutant versions (Table S1) into the luciferase reporter plasmid pGL3-Basic. In the mutant MIEPs, one or all five ACGT motifs were changed to CTAG. Using a luciferase reporter assay, we measured MIEP activity in WT, *Ire1* ko and *Xbp1* ko fibroblasts. As shown in Fig. 7A, MIEP activity was strongly reduced in *Ire1* ko cell but was not significantly altered in *Xbp1* ko cells. This result is consistent with the MCMV replication defect observed in *Ire1*, but not *Xbp1* ko cells (Fig. 3B). MIEP activity was not reduced in *Xbp1*/*Ire1* dko cells compared to the parental *Xbp1* ko cell (Fig. 7B), but was significantly reduced in *Atf6*/*Xbp1* dko cells compared to the parental *Atf6* ko cells (Fig. 7C). Again, the MIEP activities were consistent with the results of the viral replication kinetics (Figs. 5B and 6D). Thus, we concluded that activation of the MCMV MIEP correlated with viral replication in the same cells. We also found that the activity of the MIEP had a substantially reduced activity when all 5 ACGT motifs were mutated (Fig. 7A-C).

Next we tested whether XBP1s and ATF6(N), the active form of ATF6, can activate the MCMV MIEP and whether XBP1u can repress it. To assess the contribution of endogenous levels of the TFs, *Xbp1* ko, *Atf6* ko, and *Xbp1*/*Atf6* dko cells were used. In *Xbp1* ko cells, MIEP activity was slightly increased by expression of XBP1s, but substantially reduced by XBP1u. XBP1u also antagonized XBP1s in a dose-dependent manner (Fig. 7D). A similar result was obtained in *Atf6*$^{-/-}$ cells: MIEP activity was slightly increased by expression of ATF6(N), but substantially reduced by XBP1u. XBP1u also antagonized ATF6(N) in a dose-dependent manner (Fig. 7E). In *Atf6*/*Xbp1* dko cell, expression of either XBP1s or ATF6(N) was sufficient to increase MIEP activity substantially. XBP1u alone did

bioRxiv preprint doi: https://doi.org/10.1101/763227; this version posted September 9, 2019. The copyright holder for this preprint (which was not certified by peer review) is the author/funder. All rights reserved. No reuse allowed without permission.

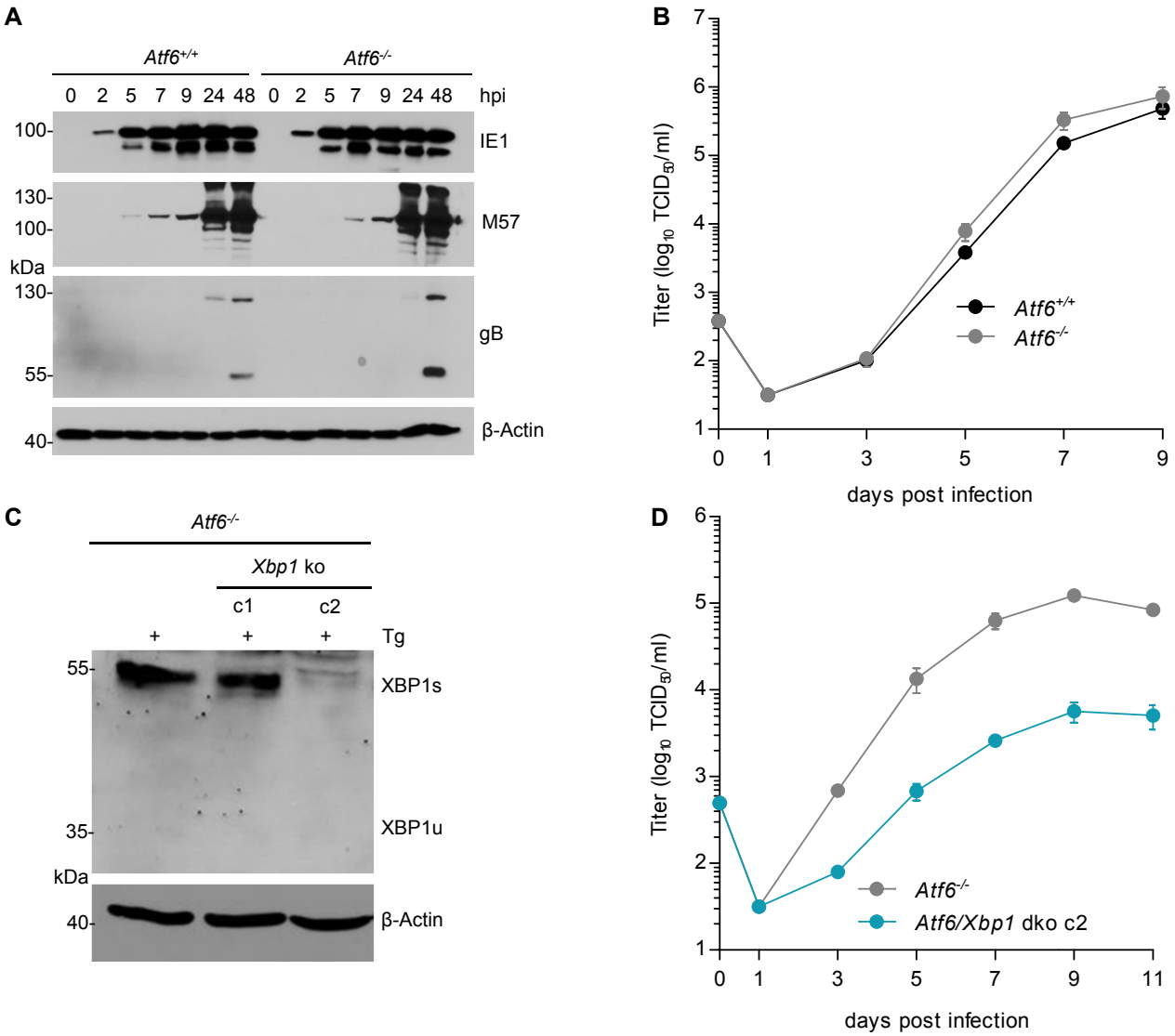

Figure 6.

MCMV replication is impaired in cells lacking *Atf6* and *Xbp1*.

A. Immunoblot analysis of viral gene expression of *Atf6*$^{+/+}$ and *Atf6*$^{-/-}$ cells infected with MCMV-GFP at an MOI of 3 $TCID_{50}$/ml. At indicated times cells were lysed and stained for the immediate-early 1 protein (IE1), the major DNA binding protein (M57; early gene) and glycoprotein B (gB; late gene) by immunoblot. β-Actin served as loading control.

B. Multistep replication kinetics. *Atf6*$^{+/+}$ and *Atf6*$^{-/-}$ cells were infected with MCMV-GFP at an MOI of 0.1 $TCID_{50}$/ml. Virus titers in the supernatants were determined by titration and are shown as means ±SEM of triplicates.

C. Knockout of *Xbp1* in *Atf6*$^{-/-}$ cells using CRISPR/Cas9 gene editing. Two single cell clones generated by two individual gRNAs (c1 and c2) were analyzed for XBP1s and XBP1u expression by immunoblot. 4h prior to harvesting, cells were stimulated with thapsigargin (Tg) to enhance XBP1 expression. The parental *Atf6*$^{-/-}$ cells are shown as control.

D. Multistep replication kinetics of *Atf6*/*Xbp1* dko cells (clone c2). MCMV infection and titration was done as described in B.

bioRxiv preprint doi: https://doi.org/10.1101/763227; this version posted September 9, 2019. The copyright holder for this preprint (which was not certified by peer review) is the author/funder. All rights reserved. No reuse allowed without permission.

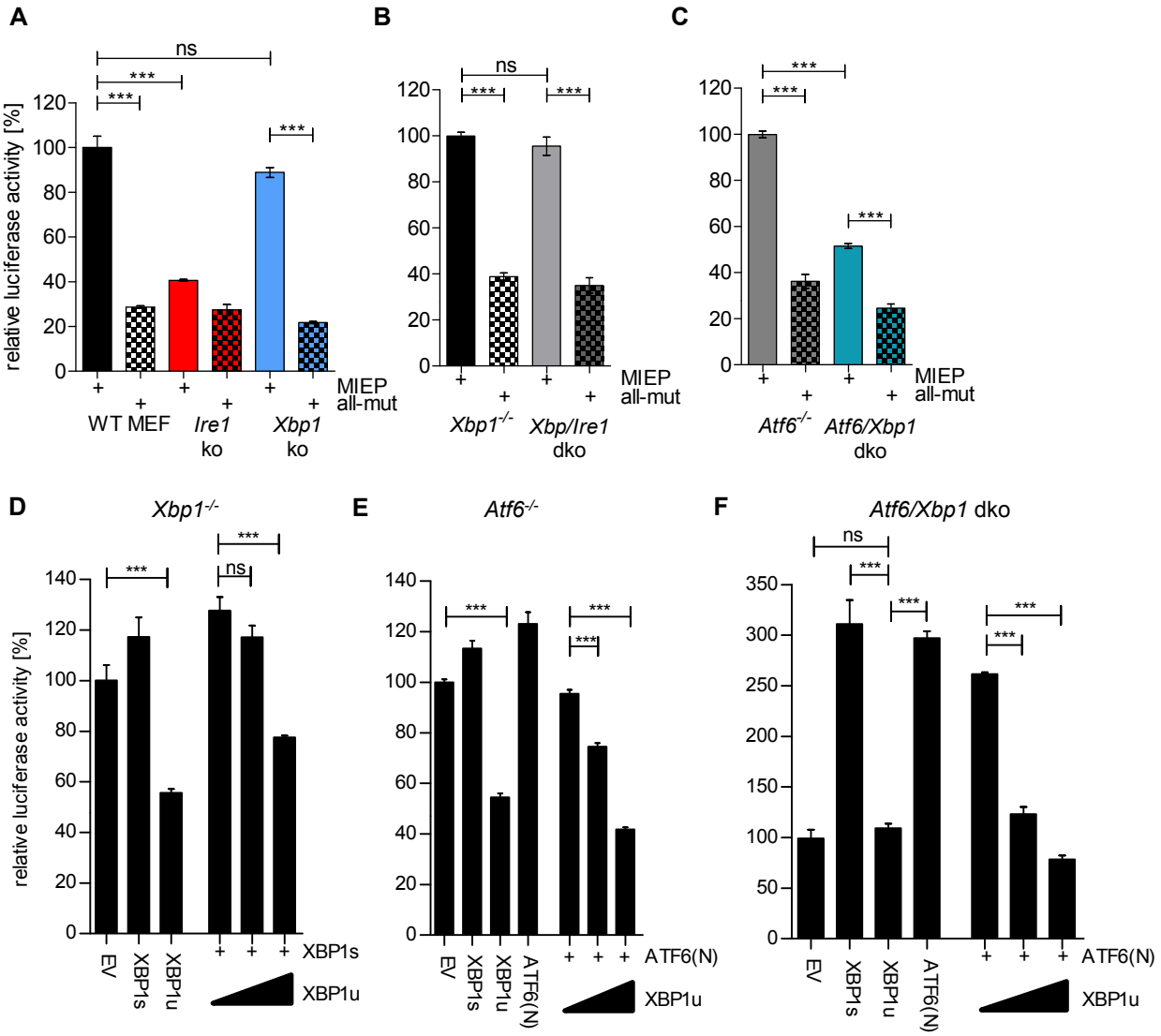

Figure 7. XBP1s and ATF6-mediated activation of the MCMV MIEP is repressed by XBP1u.

A WT MEFs, *Ire1* ko and *Xbp1* ko cells were transfected with a firefly luciferase vector containing either the WT major immediate-early promotor (MIEP) or a MIEP with 5 mutated ACGT motifs (all-mut). Renilla luciferase was expressed by co-transfection and used for normalization. Relative luciferase activities (firefly : renilla) ±SEM of 3 biological replicates are shown.

B *Xbp1*$^{-/-}$ and *Xbp1/Ire1* dko cells were transfected as in A and the relative luciferase activity was determined.

C *Atf6*$^{-/-}$ and *Atf6/Xbp1* dko cells were transfected as in A and the relative luciferase activity was determined.

D *Xbp1*$^{-/-}$ MEFs were co-transfected with firefly and renilla luciferase vectors as in A. Expression vectors for XBP1s, XBP1u, ATF6(N), or empty vector (EV) were co-transfected. Relative luciferase activities (firefly : renilla) ±SEM of 3 biological replicates are shown.

E *Atf6*$^{-/-}$ cells were transfected as in D and the relative luciferase activity was determined.

F *Atf6/Xbp1* dko cells were transfected as in A and the relative luciferase activity was determined.

bioRxiv preprint doi: https://doi.org/10.1101/763227; this version posted September 9, 2019. The copyright holder for this preprint (which was not certified by peer review) is the author/funder. All rights reserved. No reuse allowed without permission.

not reduce MIEP activity in these cells, but it antagonized the activity of ATF6(N) expressed by transfection (Fig. 7F). Taken together, these results suggest that both, XBP1s and ATF6(N), can activate the MCMV MIEP in a largely redundant fashion, and that XBP1u represses the activity of both, XBP1s and ATF6(N).

Motif 4 is necessary and sufficient for MIEP activation by XBP1s and ATF6(N).

As a first step to determine, which of the five ACGT motifs function as XBP1s and/or ATF6(N) binding sites for promoter activation, we measured the binding of these TFs to portions of the MIEP by using a DNA-protein interaction ELISA (DPI-ELISA, (Brand et al, 2010; Underwood et al, 2013). Microtiter plates were coated with double-stranded oligonucleotides encoding three copies (27 nucleotides each) of a putative binding motif with adjacent sequences on either side (Table S3). A known XBP1 binding motif of the ERdj4 promoter (Kanemoto et al, 2005) served as positive control and a sequence of the SV40 origin of replication as negative control. The oligonucleotides were incubated with HA-tagged XBP1s, XBP1u, or ATF6(N) (Fig. 8A), and DNA binding was quantified by ELISA. Mutated TFs lacking the DNA-binding domain (ΔDBD) served as negative controls. In this DPI-ELISA, XBP1s and XBP1u showed the strongest interaction with motifs 3 and 4, whereas ATF6(N) interacted with motifs 2 and 4 (Fig. 8B).

Next we used the luciferase reporter assay to test which of the five motifs was required for MIEP activation by XBP1s and ATF6(N). We used five mutants MIEPs having one of the ACGT motifs changed to CTAG. These reporter plasmids were transfected into *Atf6*/*Xbp1* dko cells, together with expression plasmids for XBP1s, XBP1u, and ATF6(N). As shown in Fig. 9A, XBP1s or ATF6(N) expression increased the activity of all MIEP constructs except MIEP-4mut and MIEP-all-mut, indicating that ACGT motif 4 is necessary for MIEP activation by XBP1s and ATF6(N).

Finally, we tested whether motif 4 was also sufficient for MIEP activation by XBP1s and ATF6(N). Motif 4 was restored in MIEP-all-mut to generate a MIEP containing only ACGT motif 4 (MIEP-4only, Table S1). Indeed, MIEP-4only was inducible by XBP1s and ATF6(N) (Fig. 9B), suggesting that motif 4 is sufficient to confer MIEP responsiveness to XBP1s and ATF6.

Taken together, the results of this study show that MCMV transiently activates the IRE1-XBP1 signaling pathway in the early phase of infection in order to relieve XBP1u-mediated repression of viral gene expression and replication. The MCMV major immediate-early promoter requires XBP1s or ATF6(N) for full activation, and XBP1u represses the activity of both TFs. Thus, XBP1u acts as a key repressor of two UPR pathways, the IRE1-XBP1 and the ATF6 pathways, which have overlapping and redundant functions.

bioRxiv preprint doi: https://doi.org/10.1101/763227; this version posted September 9, 2019. The copyright holder for this preprint (which was not certified by peer review) is the author/funder. All rights reserved. No reuse allowed without permission.

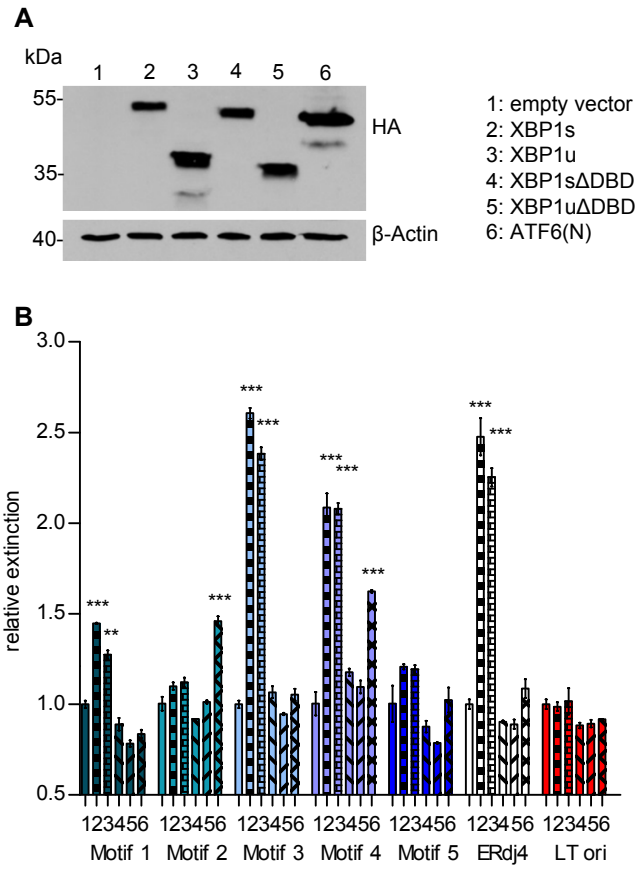

Figure 8. Transcription factor binding the MIE promotor

A. HEK 293A cells were transfected with expression vectors encoding HA-tagged WT or mutant XBP1 and ATF6(N) transcription factors. Nuclear extracts were obtained, and transcription factor expression was verified by immunoblot analysis.

B. Microtiter plates coated with dsDNA oligonucleotides containing XBP1 core binding motifs from the MCMV major immediate-early promoter, the ERdj4 promoter (positive control) or an unrelated sequence from the SV40 origin of replication (negative control). Wells were incubated with nuclear extracts 1 to 6 shown in A, and transcription factor binding was measured by DPI-ELISA, and values were normalized to extract 1 (empty vector). Means ±SEM of triplicates are shown. **, $p<0.01$; ***, $p<0.001$.

bioRxiv preprint doi: https://doi.org/10.1101/763227; this version posted September 9, 2019. The copyright holder for this preprint (which was not certified by peer review) is the author/funder. All rights reserved. No reuse allowed without permission.

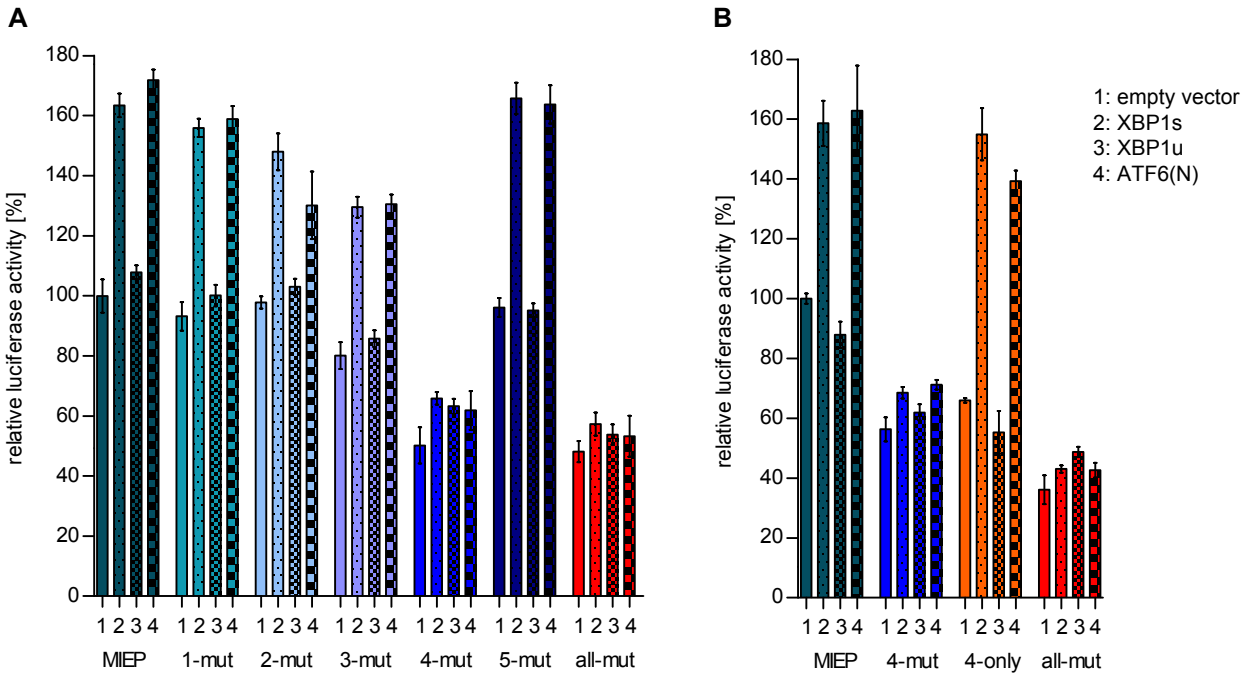

Figure 9. Motif 4 is necessary and sufficient for MIEP activation by XBP1s and ATF6(N).

A *Atf6/Xbp1* dko MEFs cells were transfected with a firefly luciferase vector containing either the WT major immediate-early promotor (MIEP) or a MIEP with 1 or all ACGT motifs mutated. Expression vectors for XBP1a, XBP1u, ATF6(N), or empty vector (EV) were co-transfected. Renilla luciferase was expressed by co-transfection and used for normalization. Relative luciferase activities (firefly : renilla) ±SEM of 3 biological replicates are shown.

B *Atf6/Xbp1* dko MEF cells were transfected and analyzed as in A. In addition, a MIEP vector with all ACGT motifs mutated except motif 4 (4-only) was included.

bioRxiv preprint doi: https://doi.org/10.1101/763227; this version posted September 9, 2019. The copyright holder for this preprint (which was not certified by peer review) is the author/funder. All rights reserved. No reuse allowed without permission.

Discussion

This study shows how MCMV harnesses UPR signaling to regulate its own life cycle. The viral MIEP, the key promotor of the lytic replication cycle, contains five ACGT motifs, of which motif 4 is most important for MIEP activation by XBP1s or ATF6(N) (Fig. 9). The fact that MIEP activity and viral replication are virtually unaffected in the absence of either XBP1 or ATF6 but are massively reduced in the absence of both, strongly suggests that the two UPR TFs have redundant roles in the activation of the MIEP. The most important finding, however, is the dominant role of XBP1u as a repressor of viral gene expression and replication. When IRE1 is absent or its RNase activity is blocked, XBP1u dominates and prevents MIEP activation by XBP1s and ATF6(N). Thus, the transient activation of IRE1 during the early phase of MCMV infection serves the virus by increasing XBP1s and decreasing XBP1u expression, thereby relieving XPB1u-mediated repression.

How exactly XBP1u antagonizes XBP1s and ATF6(N)-mediated promoter activation, remains to be determined. Two possible mechanisms may be involved: XBP1u could interact with XBP1s and ATF6(N) and target them for proteasomal degradation as previously reported (Yoshida et al, 2006; Yoshida et al, 2009). Additionally, XBP1u could bind directly to DNA and inhibit promoter activation by XBP1s and ATF6(N). Indeed, we show that XBP1u is fully capable of binding to the same DNA sequences that XBP1s binds to (Fig. 8). Moreover, a truncated XBP1 protein, XBP1stop, which lacks the C-terminal destabilizing domain of XBP1u, had a similar repressive effect as XBP1u (Fig 5D) indicating that destabilization is not required for repression.

Ever since its discovery, the importance of XBP1u has been the subject of controversy. In yeast, the unspliced mRNA of HAC1, the yeast homolog of XBP1, is posttranscrptionally silenced, and a protein product of the unspliced HAC1 mRNA has not been detected (Ruegsegger et al, 2001). In mammalian cells, the XBP1u protein is readily detectable, but XBP1u has a short half-life (Navon et al, 2010; Tirosh et al, 2006). This has led to the conclusion that XBP1u is of minor importance and its function restricted to fine-tuning of the UPR (Byrd & Brewer, 2012). Hence, many review articles on the UPR barely mention XBP1u. On the other hand, XBP1u has been shown to dimerize with XBP1s and ATF6(N) and destabilize them (Yoshida et al, 2006; Yoshida et al, 2009), suggesting a more important regulatory role. However, the physiological relevance of these findings has been called into question by some scientists because the findings were made in cells overexpressing XBP1u. The results of our study show that XBP1u plays a very important role as a repressor of XBP1s and ATF6(N)-mediated activation of the MCMV MIEP, which results in a massively (~100-fold) reduced production of progeny virus (Figs. 2, 3B, and 5D). In IRE1 ko cells, the XBP1 transcript is expressed from its endogenous promoter, not from a strong heterologous promoter. Thus, the observed effects cannot be dismissed as overexpression

bioRxiv preprint doi: https://doi.org/10.1101/763227; this version posted September 9, 2019. The copyright holder for this preprint (which was not certified by peer review) is the author/funder. All rights reserved. No reuse allowed without permission.

artifacts. Moreover, the fact that MCMV replication is massively reduced in IRE1 ko cells (Figs. 2 and 3B), but not in IRE1/XBP1 dko cells (Fig. 5B), demonstrates that XBP1u expression rather than the absence RIDD is responsible for the observed effect. Hence, the data of our study suggest that XBP1u plays an unexpectedly important role as a repressor, at least under the conditions of viral infection. Whether XBP1u can repress expression of cellular genes in a similar fashion is an important question that needs to be answered in future studies.

XBP1 binding sites have also been identified in immediate-early gene promoters of the γ-herpesviruses Epstein-Barr virus, Kaposi's sarcoma-associated herpesvirus, and murine gammaherpesvirus 68 (MHV-68), suggesting a potential role for XBP1s in transactivating these promoters during reactivation from latency (Bhende et al, 2007; Matar et al, 2014; Sun & Thorley-Lawson, 2007; Wilson et al, 2007; Yu et al, 2007). However, one study demonstrated that XBP1 was not required for MHV-68 reactivation in B cells (Matar et al, 2014). The authors of the study speculated that the apparent independence of MHV-68 reactivation from XBP1 expression in B cells might reflect redundancy among CREB/ATF family TFs. In light of our data showing a redundancy of XBP1s and ATF6(N) in the activation of the MCMV MIEP, this speculation may well be correct. Conversely, it would be interesting to know whether XBP1 and ATF6 also regulate MCMV reactivation from latency. Unfortunately, this obvious question is difficult to address as there is no manageable experimental system for MCMV latency and reactivation. Nonetheless, it appears likely that β and γ-herpesviruses harness UPR TFs in a similar fashion to regulate their life cycle.

Materials and Methods

Cells and viruses

The following immortalized fibroblast lines were used: wildtype MEFs (Manzl et al, 2009), 10.1 cells (Harvey & Levine, 1991), *Xbp1*$^{-/-}$ MEFs (Reimold et al, 2000), Primary *Atf6*$^{+/+}$ and *Atf6*$^{-/-}$ MEFs (Wu et al, 2007) were kindly provided by D. Thomas Rutkowski (University of Iowa, USA). They were immortalized by transduction with a retroviral vector encoding SV40 large T antigen (pBABE-zeo largeTcDNA, Addgene). The *Atf6*$^{+/+}$ vs. *Atf6*$^{-/-}$ state was verified by PCR as described (Wu et al, 2007). TetON-IRE1-GFP MEFs were obtained by reconstituting *Ire1*$^{-/-}$ MEFs with GFP-tagged murine IRE1 under control of a 'tight' Tet-responsive element (Clontech) essentially as described (Bakunts et al, 2017; Cohen et al, 2017). The GFP tag was introduced into the juxtamembrane cytosolic linker domain of IRE1, where such tagging had been shown before to not interfere with function of human IRE1 (Li et al, 2010). All cells were grown under standard conditions in Dulbecco´s modified Eagle´s

bioRxiv preprint doi: https://doi.org/10.1101/763227; this version posted September 9, 2019. The copyright holder for this preprint (which was not certified by peer review) is the author/funder. All rights reserved. No reuse allowed without permission.

medium supplemented with 10% fetal calf serum or 10% fetal calf serum tetracycline-free, 100 IU/ml penicillin and 100 µg/ml streptomycin (Sigma).

MCMV-GFP (Brune et al, 2001) was propagated and titrated on 10.1 fibroblasts. Viral titers were determined by using the median tissue culture infective dose ($TCID_{50}$) method. Virus was inactivated by 254-nm-wavelength UV irradiation with 1 J/cm^2 for 30 s using a UV cross-linker (HL-2000 HybriLinker; UVP).

Plasmids and transfection

XBP1-wt and XBP1-unsplicable cDNAs (Tirosh et al, 2006) were cloned in pcDNA3. The XBP1-wt vector was used to generate by PCR an XBP1stop mutant consisting of only the N-terminal domain of XBP1. The XBP1s cDNA was generated by isolating RNA from MEFs stimulated with tunicamycin (Sigma), reverse transcription, and PCR amplification. To generate XBP1-unsplicable and XBP1-spliced plasmids lacking the DNA-binding domain (ΔDBD) the complete DBD was replaced by an alternative NLS sequence as previously described (Zhou et al, 2011). Transcripts of XBP1 proteins were HA-tagged by PCR amplification and subcloned in pMSCVpuro (Clonetech), a retroviral vector plasmid. Similarly, mIRE1-wt was PCR-amplified (without a myc tag) from pcDNA3-mIRE1-3xmyc (Stahl et al, 2013) and subcloned in pMSCVhyg (Clontech) using BglII and HpaI sites. The K907A mutation was introduced by QuikChange site-directed mutagenesis (Stratagene). Transient transfection was done using GenJet (SignaGen) or polyethylenimine (Sigma).

Retroviral transduction and CRISPR/Cas9 gene editing

Retrovirus production using the Phoenix packaging cell line and transduction of target cells was done as described (Swift et al, 2001). Cells transduced with MSCVpuro and MSCVhyg vectors were selected with 1.5 µg/ml puromycin (Sigma) or 50 µg/ml hygromycin B (Roth), respectively.

Guide RNAs (Table S2) for genes of interest were designed using the online tool E-CRISP (http://www.e-crisp.org/E-CRISP/designcrispr.html) and inserted into the lentiviral vector pSicoR-CRISPR-puroR (kindly provided by R. J. Lebbink, University Medical Center Utrecht, Netherlands). Lentiviruses were produced in 293T cells using standard third-generation packaging vectors as described (van Diemen et al, 2016). Lentiviruses were used to transduce MEFs in the presence of polybrene (5 µg/ml). Cells were selected with 1.5 µg/ml puromycin and single cell clones were obtained by limiting dilution.

bioRxiv preprint doi: https://doi.org/10.1101/763227; this version posted September 9, 2019. The copyright holder for this preprint (which was not certified by peer review) is the author/funder. All rights reserved. No reuse allowed without permission.

Immunoblot analysis

Whole cell lysates were obtained by lysing cells in RIPA buffer supplemented with a cOmplete™, Mini protease inhibitor cocktail (Roche). XBP1s, XBP1u, and ATF6(N) were extracted from cells treated with thapsigargin (Sigma) using a nuclear extraction protocol (Stahl et al, 2013). Insoluble material was removed by centrifugation. Protein concentrations were measured using a BCA assay (company). Equal protein amounts were boiled in sample buffer and subjected to SDS-PAGE and semi-dry blotting onto nitrocellulose membranes. For immunodetection, antibodies against the following epitopes were used: HA (16B12, BioLegend), β-actin (AC-74, Sigma), XBP1 (M-186, Santa Cruz), IRE1 (14C10, Cell Signaling), TRAF2 (Cell Signaling), and GFP (Roche). Antibodies against MCMV IE1 (CROMA101), M57, and M55/gB (SN1.07) were provided by Stipan Jonjic (University of Rijeka, Croatia). Secondary antibodies coupled to horseradish peroxidase (HRP) were purchased from Dako.

RNA isolation and quantitative PCR

Total RNA was isolated from MEFs using an innuPREP RNA Mini Kit (Analytik-Jena). Reverse transcription and cDNA synthesis was carried out with 2 µg RNA using 200 U RevertAid H Minus Reverse Transcriptase, 100 pmol Oligo$(dT)_{18}$, and 20 U RNase inhibitor (Thermo Fisher Scientific). Quantitative real-time PCR reactions employing SYBR Green were run in an 7900HT Fast Real-Time PCR System (Applied Biosystems). The following primers were used: 5′-GAGTCCGCAGCAGGTG-3′ and 5′-GTGTCAGAGTCCATGGGA-3′ for *Xbp1s*, 5′-GTGTCAGAGTCCATGGGA-3′ and 5′-GTGTCAGAGTCCATGGGA-3′ for X*bp1u, and* 5′-CCCACTCTTCCACCTTCGATG-3′ and 5′-GTCCACCACCCTGTTGCTGTAG-3′ for *Gapdh*. Reactions were performed under the following conditions: 45 cycles of 3 sec at 95°C and 30 sec at 60°C. Three replicates were analyzed for each condition, and the relative amounts of mRNAs were calculated from the comparative threshold cycle (Ct) values by using *Gapdh* as reference.

Replication kinetics

Cells were seeded in 6-well plates and infected by an MOI of 3 or 0.1 for single or multi-step replication kinetics, respectively. Six hpi the medium was exchanged to remove the inoculum. Supernatant samples were harvested at different times post infection, and viral titers were determined on 10.1 fibroblasts using the $TCID_{50}$ method.

MIE promotor activity assay

The firefly luciferase reporter vector pGL3-Basic, the renilla luciferase control vector pGL4.73, and the Dual-Glo Luciferase assay system were purchased from Promega. WT

bioRxiv preprint doi: https://doi.org/10.1101/763227; this version posted September 9, 2019. The copyright holder for this preprint (which was not certified by peer review) is the author/funder. All rights reserved. No reuse allowed without permission.

and mutant versions of the MCMV MIE promotor (Table S1) were synthesized by Integrated DNA Technologies and cloned in pGL3-Basic. Cells were transfect in 6-well dishes using GenJet with pGL3-MIEP (0.5 µg), pGL4.73 (0.05 µg) and transcription factor expression plasmids. The total amount of DNA was kept constant at 3 µg by filling up with empty pcDNA3 vector. On the following day, the medium was exchanged and cells were incubated for another 24 h. Cells were harvested in lysis buffer and luciferase activity was measured using a Dual-Glo Luciferase assay and a luminescence plate reader (FLUOstar-Omega, BMG Labtech). Firefly and Renilla luciferase activities were evaluated for each sample. At least 3 biological replicates were used for each condition.

DNA-Protein Interaction ELISA (DPI-ELISA)

The DPI-ELISA was performed essentially as described in detail elsewhere (Brand et al, 2010; Underwood et al, 2013). Terminally biotinylated dsDNA oligonucleotides containing 3 copies of putative TF binding sites (Table S3) were purchased from Eurofins. Oligonucleotides were adsorbed to streptavidin-coated 96-well microtiter plates and incubated with nuclear extracts (10 µg protein) from transfected HEK 293A cells expressing the HA-tagged XBP1 or ATF6(N) proteins. Nuclear extracts were obtained as described (Stahl et al, 2013). TF binding to DNA was quantified by ELISA using an anti-HA antibody, an HRP-coupled secondary antibody, and an ABTS substrate (Roche). Absorbance at 405 nm wavelength was measured using a FLUOstar-Omega plate reader. At least 3 biological replicates were used for each condition.

Acknowledgments

We thank D. Thomas Rutkowski for providing *Atf6*$^{-/-}$ MEFs and Svenja Siebels for helpful advice on the DPI-ELISA. This study was supported by the Deutsche Forschungsgemeinschaft (BR 1730/6-1 to WB), the EU Horizon 2020 Marie Sklodowska-Curie ITN-TREATMENT (Grant 721236 to BT), the German-Israeli Foundation (Grant I-1471-414.13/2018 to BT), and Giovanni Armenise-Harvard Foundation (Career Development Award to EvA).

Author contributions

Conceptualization, FH, BT, WB; Methodology, FH, EvA; Investigation, FH; Writing—Original Draft, FH, WB; Writing—Review & Editing, FH, BT, WB; Funding Acquisition, WB; Resources, EvA, BT; Supervision, WB.

Conflict of interest

The authors declare that they have no conflict of interest.

bioRxiv preprint doi: https://doi.org/10.1101/763227; this version posted September 9, 2019. The copyright holder for this preprint (which was not certified by peer review) is the author/funder. All rights reserved. No reuse allowed without permission.

References

Alwine JC (2008) Modulation of host cell stress responses by human cytomegalovirus. *Curr Top Microbiol Immunol* **325:** 263-279

Bakunts A, Orsi A, Vitale M, Cattaneo A, Lari F, Tade L, Sitia R, Raimondi A, Bachi A, van Anken E (2017) Ratiometric sensing of BiP-client versus BiP levels by the unfolded protein response determines its signaling amplitude. *Elife* **6**

Bhende PM, Dickerson SJ, Sun X, Feng WH, Kenney SC (2007) X-box-binding protein 1 activates lytic Epstein-Barr virus gene expression in combination with protein kinase D. *J Virol* **81:** 7363-7370

Brand LH, Kirchler T, Hummel S, Chaban C, Wanke D (2010) DPI-ELISA: a fast and versatile method to specify the binding of plant transcription factors to DNA in vitro. *Plant methods* **6:** 25

Brune W, Ménard C, Heesemann J, Koszinowski UH (2001) A ribonucleotide reductase homolog of cytomegalovirus and endothelial cell tropism. *Science* **291:** 303-305

Buchkovich NJ, Maguire TG, Yu Y, Paton AW, Paton JC, Alwine JC (2008) Human cytomegalovirus specifically controls the levels of the endoplasmic reticulum chaperone BiP/GRP78, which is required for virion assembly. *J Virol* **82:** 31-39

Buchkovich NJ, Yu Y, Pierciey FJ, Jr., Alwine JC (2010) Human cytomegalovirus induces the endoplasmic reticulum chaperone BiP through increased transcription and activation of translation by using the BiP internal ribosome entry site. *J Virol* **84:** 11479-11486

Byrd AE, Brewer JW (2012) Intricately Regulated: A Cellular Toolbox for Fine-Tuning XBP1 Expression and Activity. *Cells* **1:** 738-753

Calfon M, Zeng H, Urano F, Till JH, Hubbard SR, Harding HP, Clark SG, Ron D (2002) IRE1 couples endoplasmic reticulum load to secretory capacity by processing the XBP-1 mRNA. *Nature* **415:** 92-96

Christianson JC, Ye Y (2014) Cleaning up in the endoplasmic reticulum: ubiquitin in charge. *Nature structural & molecular biology* **21:** 325-335

Cohen N, Breker M, Bakunts A, Pesek K, Chas A, Argemi J, Orsi A, Gal L, Chuartzman S, Wigelman Y, Jonas F, Walter P, Ernst R, Aragon T, van Anken E, Schuldiner M (2017) Iron affects Ire1 clustering propensity and the amplitude of endoplasmic reticulum stress signaling. *J Cell Sci* **130:** 3222-3233

bioRxiv preprint doi: https://doi.org/10.1101/763227; this version posted September 9, 2019. The copyright holder for this preprint (which was not certified by peer review) is the author/funder. All rights reserved. No reuse allowed without permission.

Dolan A, Cunningham C, Hector RD, Hassan-Walker AF, Lee L, Addison C, Dargan DJ, McGeoch DJ, Gatherer D, Emery VC, Griffiths PD, Sinzger C, McSharry BP, Wilkinson GW, Davison AJ (2004) Genetic content of wild-type human cytomegalovirus. *J Gen Virol* **85:** 1301-1312

Drori A, Messerle M, Brune W, Tirosh B (2014) Lack of XBP-1 impedes murine cytomegalovirus gene expression. *PLoS One* **9:** e110942

Harvey DM, Levine AJ (1991) p53 alteration is a common event in the spontaneous immortalization of primary BALB/c murine embryo fibroblasts. *Genes Dev* **5:** 2375-2385

Isler JA, Skalet AH, Alwine JC (2005) Human cytomegalovirus infection activates and regulates the unfolded protein response. *J Virol* **79:** 6890-6899

Kanemoto S, Kondo S, Ogata M, Murakami T, Urano F, Imaizumi K (2005) XBP1 activates the transcription of its target genes via an ACGT core sequence under ER stress. *Biochem Biophys Res Commun* **331:** 1146-1153

Lacaze P, Forster T, Ross A, Kerr LE, Salvo-Chirnside E, Lisnic VJ, Lopez-Campos GH, Garcia-Ramirez JJ, Messerle M, Trgovcich J, Angulo A, Ghazal P (2011) Temporal profiling of the coding and noncoding murine cytomegalovirus transcriptomes. *J Virol* **85:** 6065-6076

Lee K, Tirasophon W, Shen X, Michalak M, Prywes R, Okada T, Yoshida H, Mori K, Kaufman RJ (2002) IRE1-mediated unconventional mRNA splicing and S2P-mediated ATF6 cleavage merge to regulate XBP1 in signaling the unfolded protein response. *Genes Dev* **16:** 452-466

Li H, Korennykh AV, Behrman SL, Walter P (2010) Mammalian endoplasmic reticulum stress sensor IRE1 signals by dynamic clustering. *Proc Natl Acad Sci U S A* **107:** 16113-16118

Manzl C, Krumschnabel G, Bock F, Sohm B, Labi V, Baumgartner F, Logette E, Tschopp J, Villunger A (2009) Caspase-2 activation in the absence of PIDDosome formation. *J Cell Biol* **185:** 291-303

Marcinowski L, Lidschreiber M, Windhager L, Rieder M, Bosse JB, Radle B, Bonfert T, Gyory I, de Graaf M, Prazeres da Costa O, Rosenstiel P, Friedel CC, Zimmer R, Ruzsics Z, Dolken L (2012) Real-time transcriptional profiling of cellular and viral gene expression during lytic cytomegalovirus infection. *PLoS Pathog* **8:** e1002908

Matar CG, Rangaswamy US, Wakeman BS, Iwakoshi N, Speck SH (2014) Murine gammaherpesvirus 68 reactivation from B cells requires IRF4 but not XBP-1. *J Virol* **88:** 11600-11610

Maurel M, Chevet E, Tavernier J, Gerlo S (2014) Getting RIDD of RNA: IRE1 in cell fate regulation. *Trends Biochem Sci* **39:** 245-254

bioRxiv preprint doi: https://doi.org/10.1101/763227; this version posted September 9, 2019. The copyright holder for this preprint (which was not certified by peer review) is the author/funder. All rights reserved. No reuse allowed without permission.

Mocarski ES, Jr. (2002) Immunomodulation by cytomegaloviruses: manipulative strategies beyond evasion. *Trends Microbiol* **10:** 332-339

Moore K, Hollien J (2015) Ire1-mediated decay in mammalian cells relies on mRNA sequence, structure, and translational status. *Mol Biol Cell* **26:** 2873-2884

Navon A, Gatushkin A, Zelcbuch L, Shteingart S, Farago M, Hadar R, Tirosh B (2010) Direct proteasome binding and subsequent degradation of unspliced XBP-1 prevent its intracellular aggregation. *FEBS Lett* **584:** 67-73

Novoa I, Zeng H, Harding HP, Ron D (2001) Feedback inhibition of the unfolded protein response by GADD34-mediated dephosphorylation of eIF2alpha. *J Cell Biol* **153:** 1011-1022

Qian Z, Xuan B, Chapa TJ, Gualberto N, Yu D (2012) Murine cytomegalovirus targets transcription factor ATF4 to exploit the unfolded-protein response. *J Virol* **86:** 6712-6723

Reimold AM, Etkin A, Clauss I, Perkins A, Friend DS, Zhang J, Horton HF, Scott A, Orkin SH, Byrne MC, Grusby MJ, Glimcher LH (2000) An essential role in liver development for transcription factor XBP-1. *Genes Dev* **14:** 152-157

Ruegsegger U, Leber JH, Walter P (2001) Block of HAC1 mRNA translation by long-range base pairing is released by cytoplasmic splicing upon induction of the unfolded protein response. *Cell* **107:** 103-114

Smith MH, Ploegh HL, Weissman JS (2011) Road to ruin: targeting proteins for degradation in the endoplasmic reticulum. *Science* **334:** 1086-1090

Stahl S, Burkhart JM, Hinte F, Tirosh B, Mohr H, Zahedi RP, Sickmann A, Ruzsics Z, Budt M, Brune W (2013) Cytomegalovirus downregulates IRE1 to repress the unfolded protein response. *PLoS Pathog* **9:** e1003544

Stern-Ginossar N, Weisburd B, Michalski A, Le VT, Hein MY, Huang SX, Ma M, Shen B, Qian SB, Hengel H, Mann M, Ingolia NT, Weissman JS (2012) Decoding human cytomegalovirus. *Science* **338:** 1088-1093

Sun CC, Thorley-Lawson DA (2007) Plasma cell-specific transcription factor XBP-1s binds to and transactivates the Epstein-Barr virus BZLF1 promoter. *J Virol* **81:** 13566-13577

Swift S, Lorens J, Achacoso P, Nolan GP (2001) Rapid production of retroviruses for efficient gene delivery to mammalian cells using 293T cell-based systems. *Curr Protoc Immunol* **Chapter 10:** Unit 10 17C

Tirasophon W, Lee K, Callaghan B, Welihinda A, Kaufman RJ (2000) The endoribonuclease activity of mammalian IRE1 autoregulates its mRNA and is required for the unfolded protein response. *Genes Dev* **14:** 2725-2736

bioRxiv preprint doi: https://doi.org/10.1101/763227; this version posted September 9, 2019. The copyright holder for this preprint (which was not certified by peer review) is the author/funder. All rights reserved. No reuse allowed without permission.

Tirosh B, Iwakoshi NN, Glimcher LH, Ploegh HL (2006) Rapid turnover of unspliced Xbp-1 as a factor that modulates the unfolded protein response. *J Biol Chem* **281:** 5852-5860

Underwood KF, Mochin MT, Brusgard JL, Choe M, Gnatt A, Passaniti A (2013) A quantitative assay to study protein:DNA interactions, discover transcriptional regulators of gene expression, and identify novel anti-tumor agents. *Journal of visualized experiments : JoVE*

Urano F, Wang X, Bertolotti A, Zhang Y, Chung P, Harding HP, Ron D (2000) Coupling of stress in the ER to activation of JNK protein kinases by transmembrane protein kinase IRE1. *Science* **287:** 664-666

van Diemen FR, Kruse EM, Hooykaas MJ, Bruggeling CE, Schurch AC, van Ham PM, Imhof SM, Nijhuis M, Wiertz EJ, Lebbink RJ (2016) CRISPR/Cas9-Mediated Genome Editing of Herpesviruses Limits Productive and Latent Infections. *PLoS Pathog* **12:** e1005701

Walter P, Ron D (2011) The unfolded protein response: from stress pathway to homeostatic regulation. *Science* **334:** 1081-1086

Wang Y, Shen J, Arenzana N, Tirasophon W, Kaufman RJ, Prywes R (2000) Activation of ATF6 and an ATF6 DNA binding site by the endoplasmic reticulum stress response. *J Biol Chem* **275:** 27013-27020

Wilson SJ, Tsao EH, Webb BL, Ye H, Dalton-Griffin L, Tsantoulas C, Gale CV, Du MQ, Whitehouse A, Kellam P (2007) X box binding protein XBP-1s transactivates the Kaposi's sarcoma-associated herpesvirus (KSHV) ORF50 promoter, linking plasma cell differentiation to KSHV reactivation from latency. *J Virol* **81:** 13578-13586

Wu J, Rutkowski DT, Dubois M, Swathirajan J, Saunders T, Wang J, Song B, Yau GD, Kaufman RJ (2007) ATF6alpha optimizes long-term endoplasmic reticulum function to protect cells from chronic stress. *Dev Cell* **13:** 351-364

Yoshida H, Haze K, Yanagi H, Yura T, Mori K (1998) Identification of the cis-acting endoplasmic reticulum stress response element responsible for transcriptional induction of mammalian glucose-regulated proteins. Involvement of basic leucine zipper transcription factors. *J Biol Chem* **273:** 33741-33749

Yoshida H, Matsui T, Yamamoto A, Okada T, Mori K (2001) XBP1 mRNA is induced by ATF6 and spliced by IRE1 in response to ER stress to produce a highly active transcription factor. *Cell* **107:** 881-891

Yoshida H, Oku M, Suzuki M, Mori K (2006) pXBP1(U) encoded in XBP1 pre-mRNA negatively regulates unfolded protein response activator pXBP1(S) in mammalian ER stress response. *J Cell Biol* **172:** 565-575

bioRxiv preprint doi: https://doi.org/10.1101/763227; this version posted September 9, 2019. The copyright holder for this preprint (which was not certified by peer review) is the author/funder. All rights reserved. No reuse allowed without permission.

621 Yoshida H, Uemura A, Mori K (2009) pXBP1(U), a negative regulator of the unfolded protein
622 response activator pXBP1(S), targets ATF6 but not ATF4 in proteasome-mediated
623 degradation. *Cell structure and function* **34:** 1-10

624
625 Yu F, Feng J, Harada JN, Chanda SK, Kenney SC, Sun R (2007) B cell terminal
626 differentiation factor XBP-1 induces reactivation of Kaposi's sarcoma-associated herpesvirus.
627 *FEBS Lett* **581:** 3485-3488

628
629 Yu Y, Pierciey FJ, Jr., Maguire TG, Alwine JC (2013) PKR-like endoplasmic reticulum kinase
630 is necessary for lipogenic activation during HCMV infection. *PLoS Pathog* **9:** e1003266

631
632 Zhang L, Wang A (2012) Virus-induced ER stress and the unfolded protein response. *Front*
633 *Plant Sci* **3:** 293

634
635 Zhao Y, Li X, Ma K, Yang J, Zhou J, Fu W, Wei F, Wang L, Zhu WG (2013) The axis of
636 MAPK1/3-XBP1u-FOXO1 controls autophagic dynamics in cancer cells. *Autophagy* **9:** 794-
637 796

638
639 Zhou Y, Lee J, Reno CM, Sun C, Park SW, Chung J, Fisher SJ, White MF, Biddinger SB,
640 Ozcan U (2011) Regulation of glucose homeostasis through a XBP-1-FoxO1 interaction. *Nat*
641 *Med* **17:** 356-365

642

643

644